

# CAN THE EXTRACTED CHEMICAL INFORMATION FROM FFPE SAMPLES USING LA-REIMS IMAGING SUPPORT PATHOLOGICAL DIAGNOSIS?

Authors: Gabriel Stefan Horkovics-Kovats<sup>1,2</sup>; Richard Schäffer<sup>1</sup>; Csaba Hajdu<sup>1</sup>; Attila Egri<sup>1</sup>; Fanni Csiza<sup>3</sup>; Bálint András Deák<sup>3</sup>; Benedek Gyöngyösi<sup>3</sup>; Gitta Schlosser<sup>2</sup>; Julia Balog<sup>1</sup>

Affiliations: <sup>1</sup>Waters Research Center; <sup>2</sup>Eötvös Loránd University; <sup>3</sup>Department of Pathology, Forensic and Insurance Medicine Semmelweis University; Budapest, Hungary

For Research Use Only. Not for use in diagnostic procedures.  
REIMS and Xevo are trademarks of Waters Technologies Corporation

## INTRODUCTION

- According to the gold standard, all clinically collected tissue samples are stored in formalin-fixed and paraffin-embedded (FFPE) blocks
- Large archives of FFPE blocks are available worldwide and can be used for collecting molecular information from the samples
- Chemical information is lost during the sample embedding and conservation process
- Laser Assisted Rapid Evaporative Ionization Mass spectrometry is an ambient technique requiring no sample preparation which can perform chemical imaging by point-by-point laser desorption [1,2]

## AIM

Investigate the capability of LA-REIMS Imaging to extract useful chemical information in the phospholipid region (600-900 m/z) on a set of tumorous human kidney FFPE samples by performing statistical analysis.

## METHODS

- Equipment:** Laser safe, boxed LA-REIMS imaging setup with optical parametric oscillator (2940nm) and commercial motorized X-Y-Z stage (Figure 1.)
- Workflow:** Generated aerosol from target sample introduced into REIMS™ source on a XEVO™ G2-Qtof-MS (negative, sensitivity mode)
- Sample set:** 10 annotated tumorous human kidney FFPE sections (10um thick) from different patients with the same tumour type
- Analysis:** Multivariate statistics (including PCA modelling, unsupervised clustering and supervised Image classification) and cross-validation through inhouse software

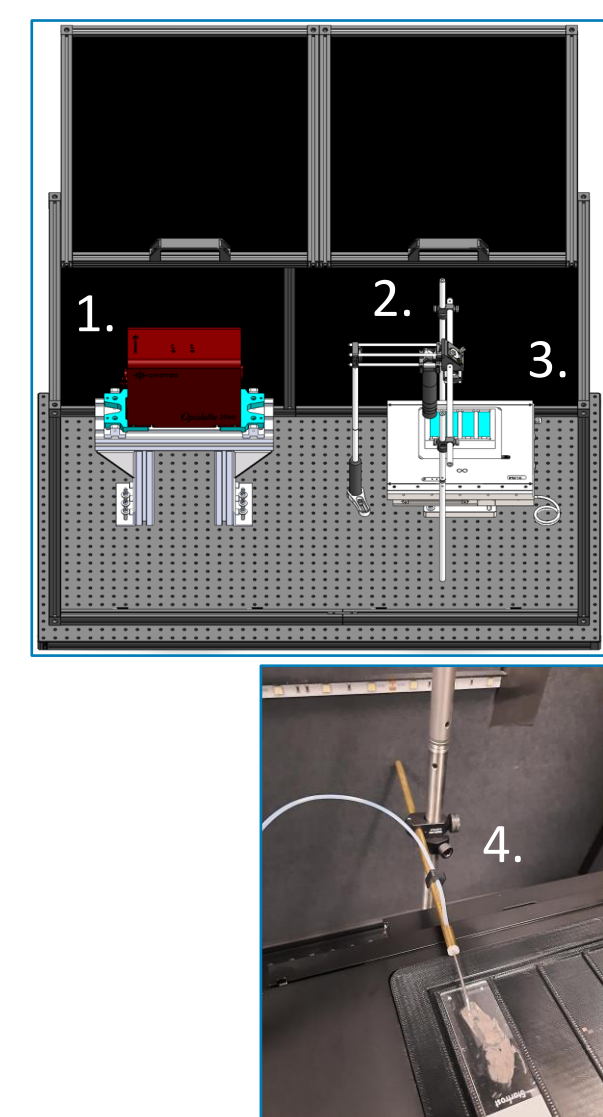


Figure 1. Laser safe, boxed LA-REIMS Imaging setup schematic and aerosol suction tube placement

- Optical parametric oscillator (OPO) used at 2940 nm
- Optical path for laser attenuation and beam focusing
- Commercial motorized X-Y-Z stage with microscope slide holder
- Aerosol suction tube placed next to the focal point of the OPO and connected to REIMS™ interface

## EXPERIMENTAL WORKFLOW

### 1. Understanding the impact of FFPE

- Taking homogenous pork liver cross section from each step of the FFPE preparation process
- Measuring samples with boxed LA-REIMS Imaging setup (Figure 1.) In order to analyse the respective qualitative and chemical differences during the procedure with spectral visualization (Figure 2), PCA model (Figure 3.) and loading plot (Figure 4.)

### 2. Data set measurement

- Sampling 10 tumorous clear cell renal cell carcinoma (ccRCC) human kidney FFPE with boxed LA-REIMS Imaging setup (Figure 1.) to see if statistically valuable results can be obtained

### 3. Image creation

- Using HDI 1.4 imaging software (Figure 5.) according to signal intensity per pixel for selected peaks and compare to pathological annotation (Figure 6.)

### 4. Unsupervised k-Nearest Neighbour (kNN) clustering

- Pathological annotation based on morphological examination
- Unsupervised kNN clustering compares all scans in one file without considering spatial location and creates corresponding images (Figure 7.)
- Chemical differences can be seen in kNN without using any class or pre-built database information
- Also serves as quality control, if no well recognizable image is generated, sample can be excluded from further model building

### 5. Model building

- Using homebuilt Abstract Model Builder (AMX) software: Creating data model by defining regions of interest (ROI) on previously created images, where statistical calculations can be performed
- ROI selection based on pathological suggestions at locations where homogeneous cell structures were encountered
- ROI classification as tumour or healthy tissue

### 6. Linear support vector classifier (LSVC)

- Using LSVC algorithm to find most important peaks for tissue differentiation
- Allows creation of peak based models, focusing only on most important features (Figure 8.)

### 7. Supervised full group out – cross validation

- Using peak-based PCA and LDA AMX models to validate the individual samples, by Full group out cross validation (Figure 9.)

### 8. Supervised image classification

- AMX recognition mode allows supervised classification using imported peak-based models, where each pixel is represented with the class calculated by the model (Figure 10.)

## RESULTS

**Understanding the impact of FFPE:** Spectra from the most important steps of the FFPE preparation process are summarized in Figure 2 below:

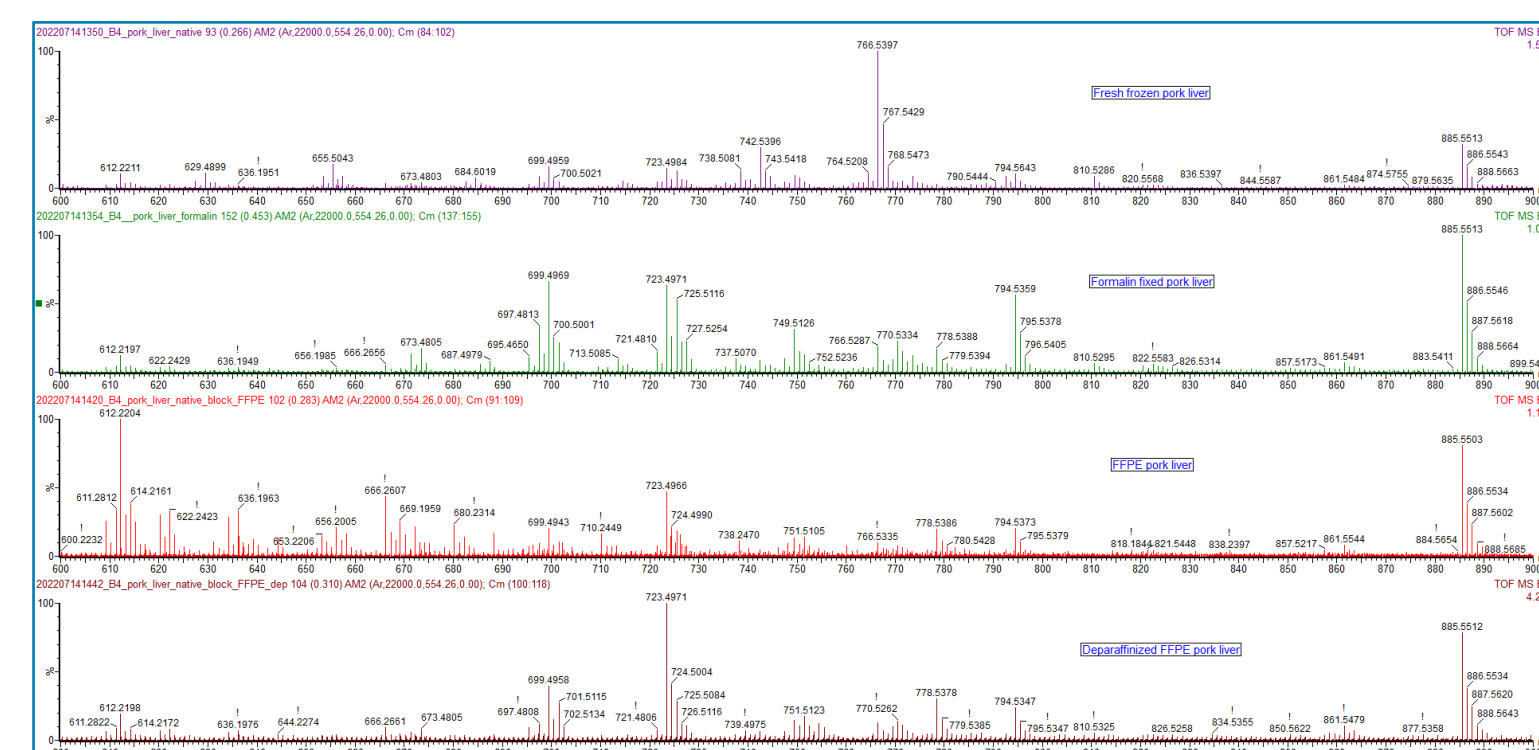


Figure 2. Leu-enk lock massed and combined spectra of 20 scans of pork liver through the FFPE creation protocol steps: Fresh frozen, formalin fixation, paraffin embedding and deparaffinization (600-900m/z)

- Across the measurements signal intensity drops by a magnitude after the formalin fixation step (Figure 2)
- Formalin fixation affects mostly 766.5 m/z - PE(38:4) and 742.5 m/z - PE(36:2) (Figure 2 and 4)
- Measuring FFPE samples reduces overall signal to noise quality
- Slight increase of the signal was observed after the deparaffinization step
- A strong decrease in the complexity of the metabolic profile is noticeable during the FFPE process

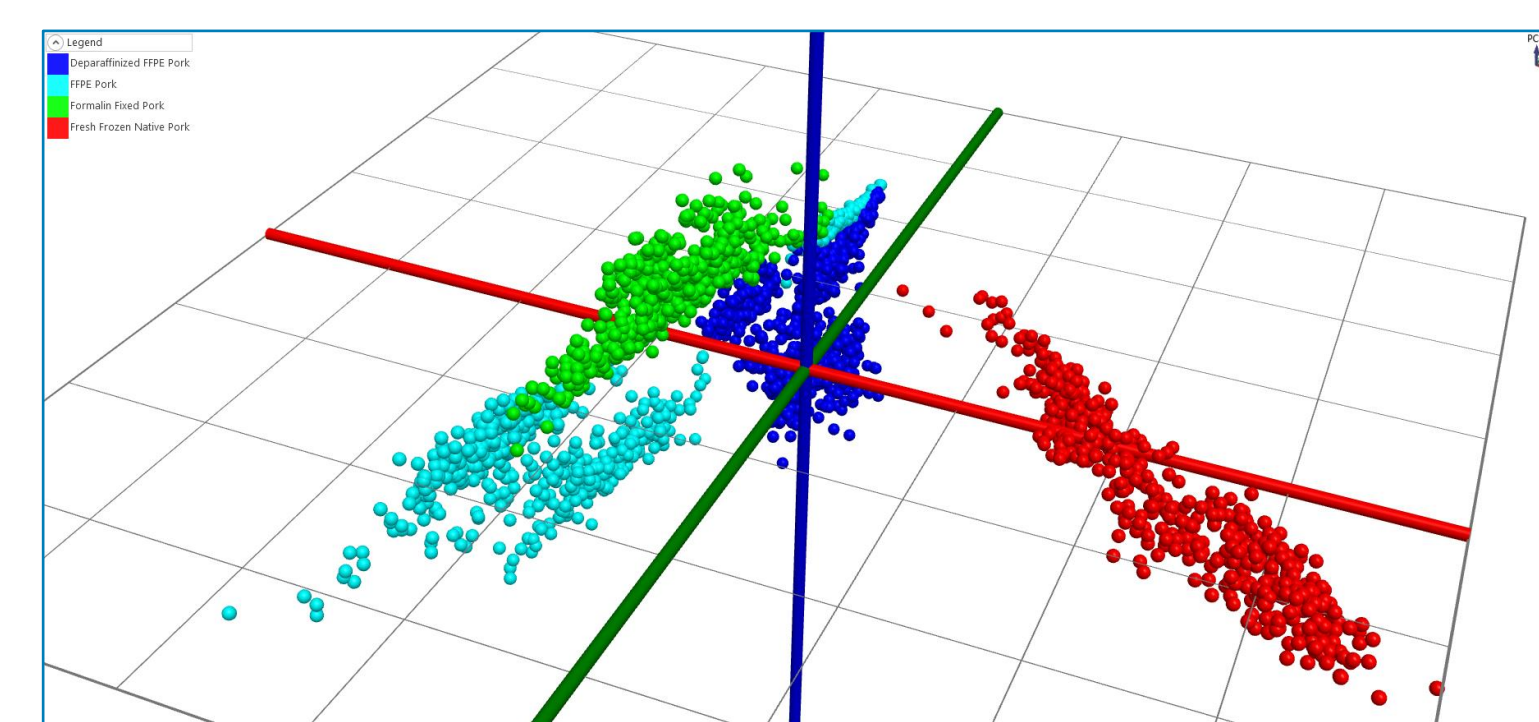


Figure 3. PCA model of Fresh frozen (red), formalin fixation (green), paraffin embedding (light blue) and deparaffinization (dark blue)

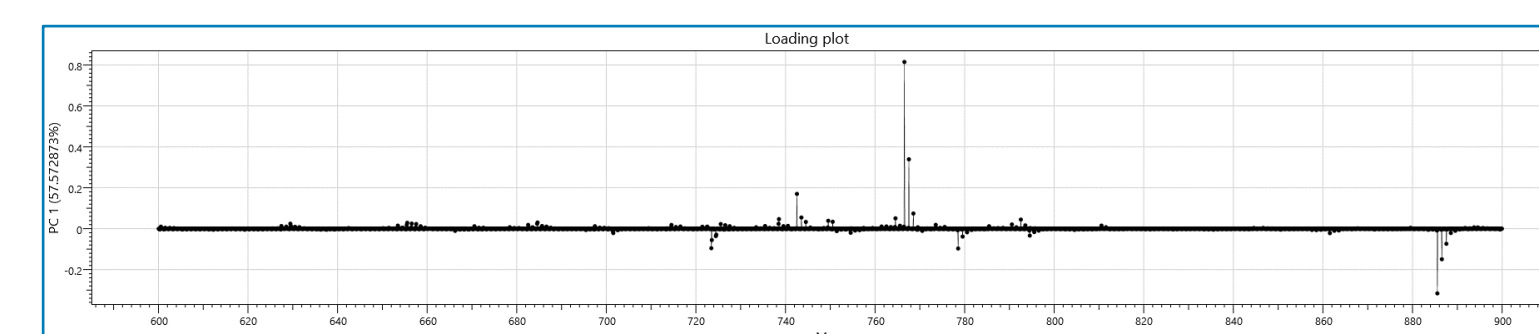


Figure 4. PC1 loading plot showing the most important peaks for tissue distinction according to PCA model

- Clear separation of four steps in PCA model
- PC1 model shows that 766.5 m/z - PE(38:4) and 742.5 m/z - PE(36:2) and 885.5 m/z - PI(28:4) have the most influence for separation in the PCA model

**Data set measurement:** For clarity reasons, the workflow is presented on only one example sample from the set.

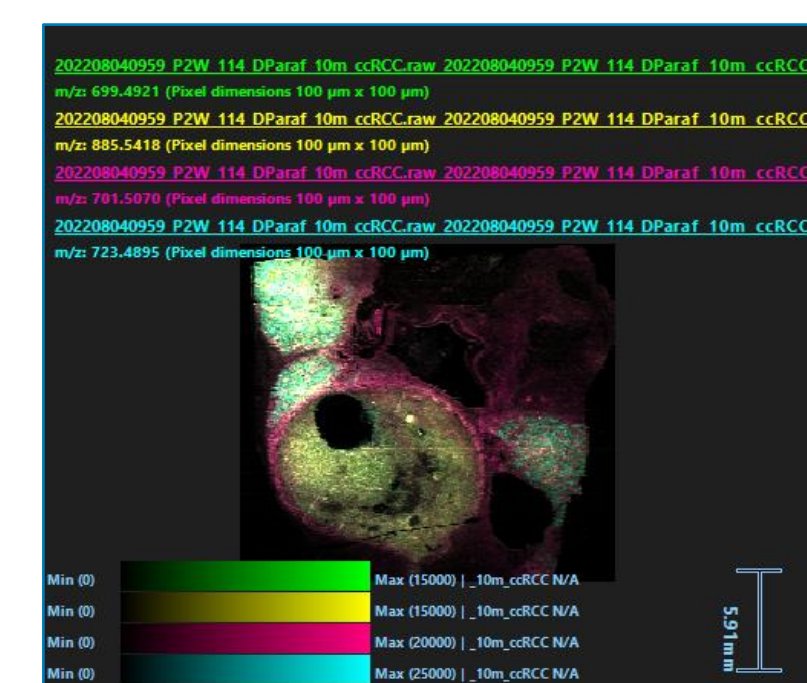


Figure 5. HDI Image with selected most prominent peaks

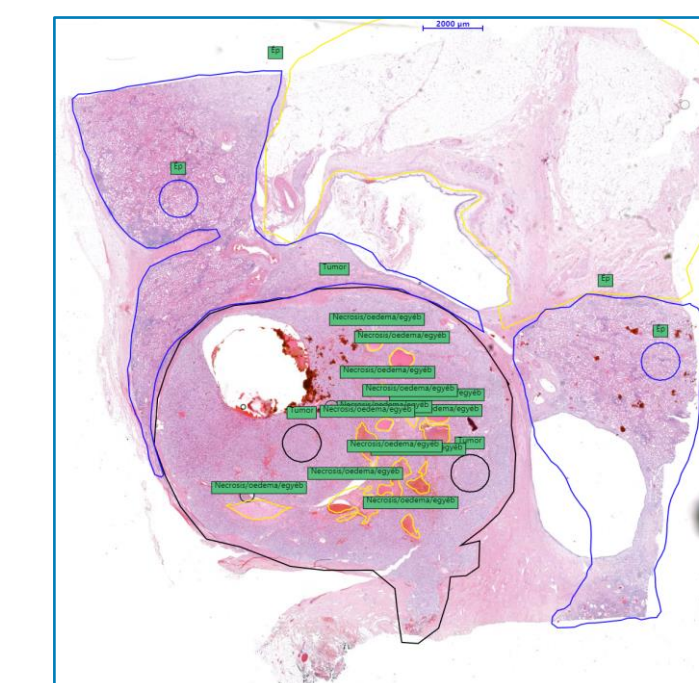


Figure 6. Pathological annotation: black (tumour), blue (healthy), yellow (necrosis)

- Good representation of the tissue in the HDI image with clear boundaries of different tissue structures
- The selected peaks alone did not replicate the pathological annotation, as they are present in different concentrations in both tumour and healthy tissue
- Homogenous regions were marked with circles in Figure 6. for further model building

### Unsupervised kNN clustering

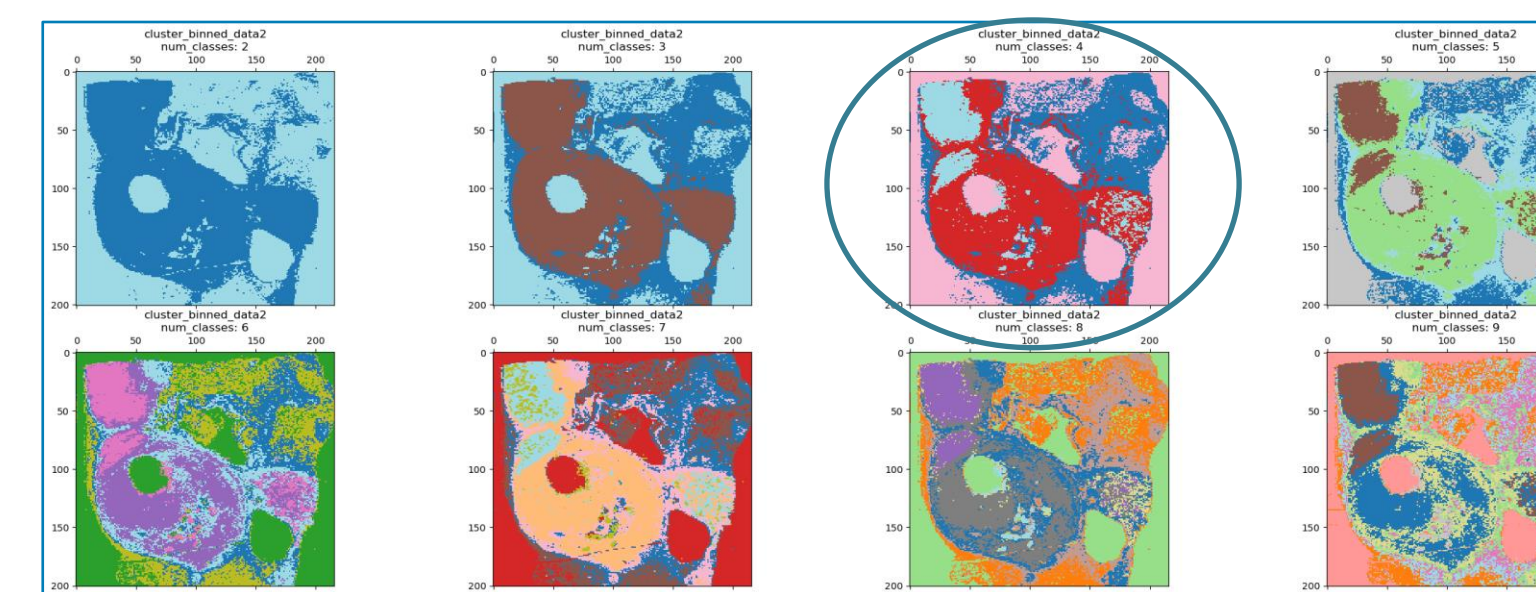


Figure 7. kNN Clustering results with 2-9 classes

- kNN achieved similar images to the HDI visualisation, especially after separation in 4 classes (Figure 7.)
- Images have no artifacts or further separation of background: Sample is usable for model building

### Model building and LSVC

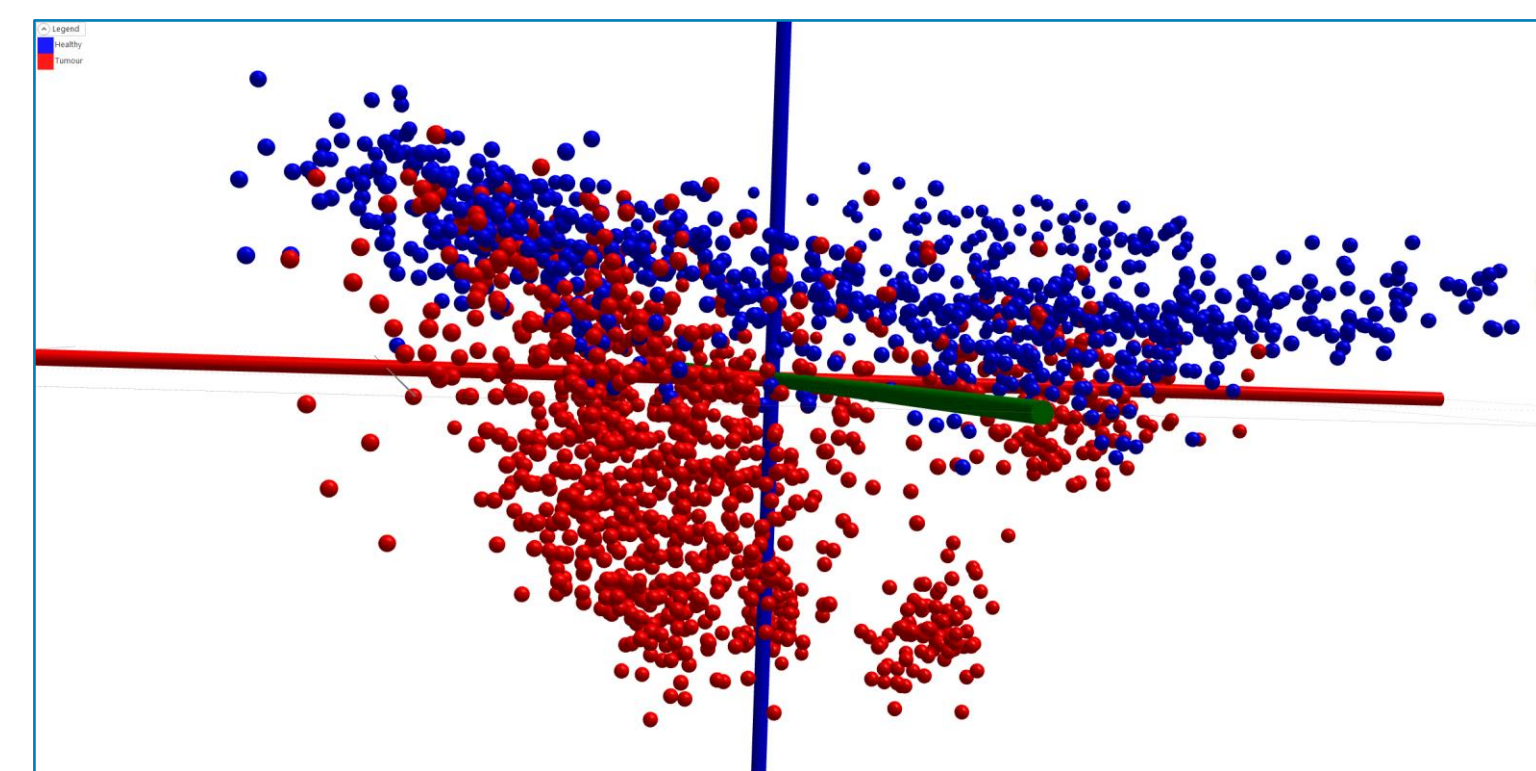


Figure 8. PCA model of whole human kidney FFPE data set created from an LSVC peak list focusing on the 600-900 m/z region with tumour scans in red and healthy scans in blue

- Separation in PCA model visible but accumulations are very close to each other and sometimes overlap

### Supervised full group out – cross validation

	healthy	tumour	Total
healthy	155	16	171
tumour	0	180	180
Total	155	196	351

Correct Classification Rate	
Excluding outliers	Including outliers
95.44%	95.44%
95.44%	95.44%

Figure 9. Confusion matrix (left) and Correct Classification Rate (Right) from showcased example sample

- Very good classification of tissue types in this example
- Correct classification rate above 90% with only 16 misclassified scans

### Supervised image classification

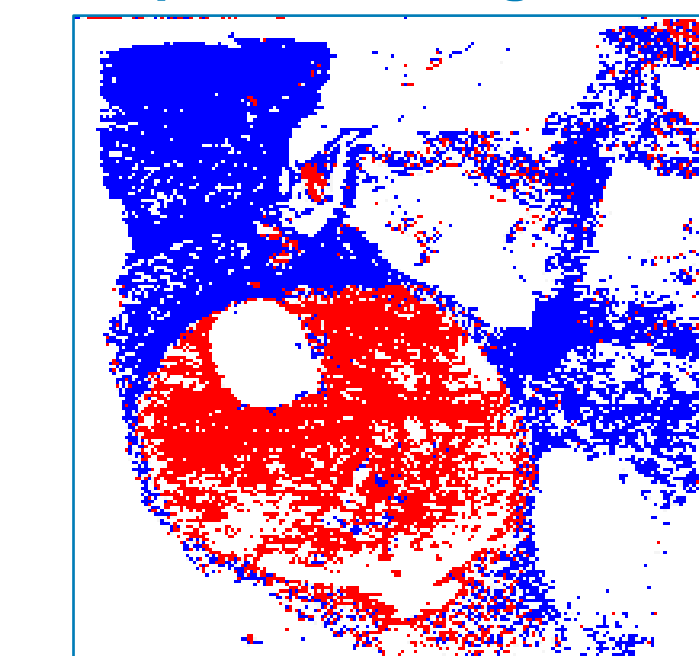


Figure 10. Supervised classification of showcased example based on previously calculated LDA classifier (AMX): Healthy tissue in blue, tumorous tissue in red and comparative image result and classification of fresh frozen mouse brain tissue

- Classification of tissue types resemble pathological annotation strongly (Figure 6.)
- Apart from the background, a lot of white artifacts are visible, showing outlier pixels indicating low quality spectra from deparaffinized FFPE samples

## RESULT SUMMARY OF DATA SET

### HDI image and annotation

- Good tissue contrast visualization through HDI possible

- Using up to 4 significant phospholipid peaks in the 600-900 m/z range for best image representation:
  - > 699.5 m/z - PE(34:1)
  - > 701.5 m/z - PE(34:0) and/or PA(36:1)
  - > 723.5 m/z - PE(36:3) and/or PA (38:4)
  - > 885.5 m/z - PI(38:4)

### Unsupervised kNN clustering

- Some similarity to the pathological annotation in 8 out of 10 samples with according class selection
- Discarding of remaining 2 samples from further model building (Table 1. sample 3 and 10)

### Supervised full group out – cross validation and image classification

Table 1. Cross validation results for every sample showcasing the correct classification rate to their representative anonymized sample number including sensitivity and specificity

Sample Nr.	1	2	3	4	5	6	7	8	9	10
Correct classification rate	51,55%	0%	/	95,44%	97,92%	61,66%	100%	48,61%	81,70%	/
Sensitivity	51,55%	n/a	/	100%	98,69%	31,32%	100%	51,97%	66,99%	/
Specificity	n/a	0%	/	90,64%	97,06%	100%	n/a	45,61%	97,89%	/

- Classification rate above 90 % for 3 out of 8 samples
- 2<sup>nd</sup> sample contained only outliers
- Wide range of classification rates: 48%-100%
- In 8 out of 8 cases supervised image classification was able to visualize tumorous and healthy regions like the pathological annotation with broad range of artifacts due to FFPE quality

## DISCUSSION

- Mass spectrometry analysis of native samples is preferred due to good signal to noise ratio and no spectral degradation:

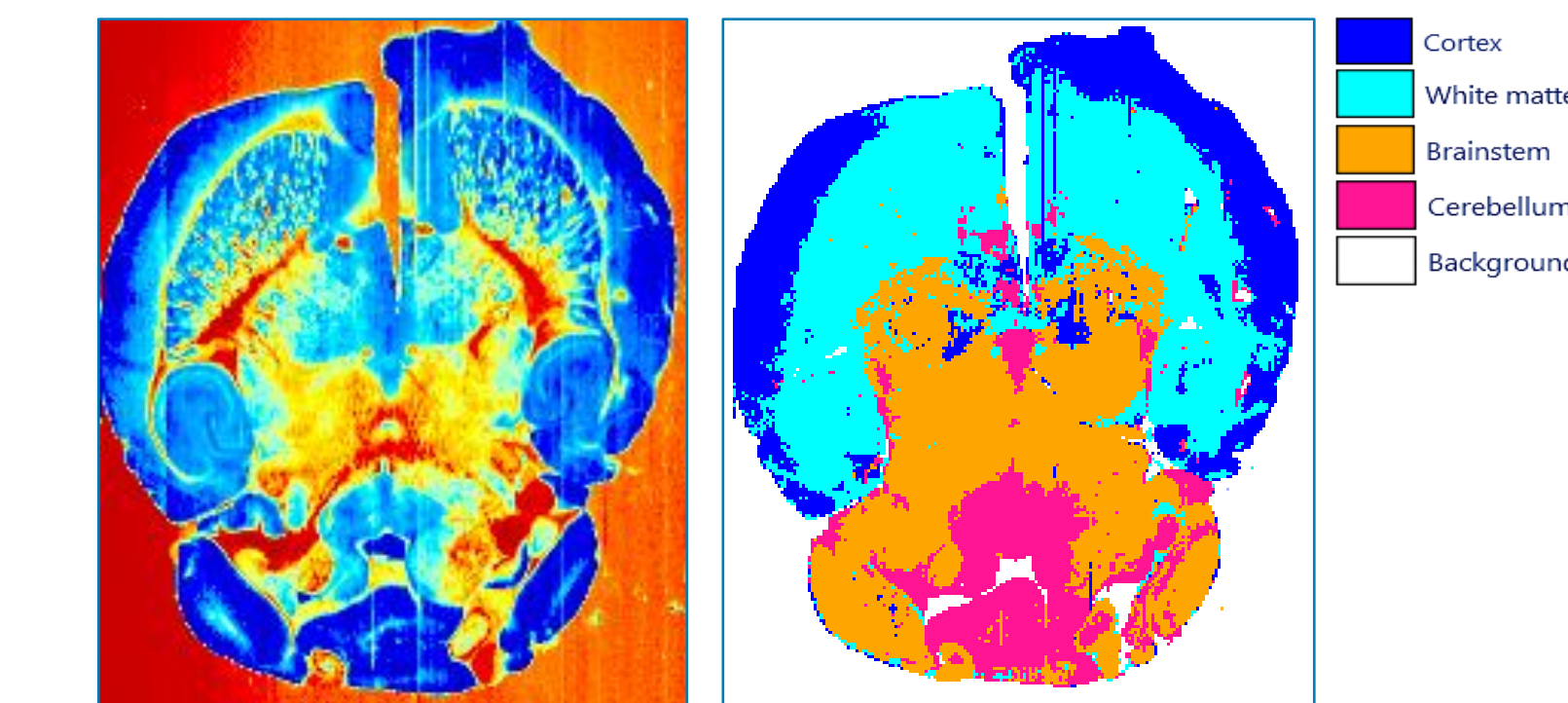


Figure 11. Comparative image result and classification of fresh frozen mouse brain tissue to represent high quality and processing possibility of fresh frozen samples using LA-REIMS imaging

- FFPE samples produced a generally poor signal-to-noise intensity and quality while sampling, caused by dehydration, lipid loss and wax embedding - also confirmed by close accumulations (Figure 8.)
- HDI image creation showed good representation of the actual tissue - Peak intensity differences clearly visible in the presented example
- Supervised classification can distinguish between tissue types for samples with sufficient signal intensity based on a pre-build database and produce an information-equivalent image compared to the pathological annotation (Images like kNN images)

## CONCLUSION

- Despite low quality of measurements on FFPE samples, imaging and statistical analysis could be performed **where possible**
- Degree of lipid flushing may vary during the creation protocol, resulting in good results for some samples and no results at all for others
- In perspective, signal amplification approaches for FFPE could be investigated, or samples simply fixed in formalin without embedding could be used to enable the acquisition of a more complex metabolic profile by mass spectrometry imaging and provide stable and reliable data for pathological analysis